NANO LETTERS

2007
Vol. 7, No. 4
1018−1021

Controlling the Growth of "Ionic" Nanoparticle Supracrystals

Alexander M. Kalsin and Bartosz A. Grzybowski*

Department of Chemical and Biological Engineering and Department of Chemistry, Northwestern University, 2145 Sheridan Road, Evanston, Illinois 60208

Received January 24, 2007; Revised Manuscript Received March 7, 2007

ABSTRACT

Dimensions and quality of supracrystals self-assembling from oppositely charged nanoparticles (NPs) can be controlled by changing the relative nanoparticle concentrations, NP polydispersity, and pH. In particular, excess nanoparticles of either polarity terminate the self-assembly process at desired stages by forming charged, stabilizing shells around the growing aggregates. In this way, average supracrystal sizes can be varied from several micrometers down to tens of nanometers. While larger crystals precipitate from the growing solution, those smaller than ca. 400 nm are soluble. The experimentally observed threshold size for solubility agrees with arguments based on the DLVO theory.

Self-assembly of charged, nanoscopic objects into larger, ordered architectures is an attractive route to new types of nanostructured materials[1] with potential applications in optoelectronics,[2] high-density data storage,[3] catalysis,[4] and biological sensing,[5] to name just a few. We have recently demonstrated the feasibility of this approach by assembling charged metallic nanoparticles into three-dimensional supracrystals, each composed of several millions of NPs[6] (Figure 1a). These initial experiments posed intriguing questions regarding both the fundamental nature of the electrostatic forces at the nanoscale[6,7] and the ability to control the properties/dimensions of the suprastructures into which charged NPs self-assemble. Here, we focus on the latter issue and investigate how the changes in the relative concentrations and the properties of the oppositely charged NPs affect the dimensions and quality of the supracrystals these nanoparticles form. We show that, by increasing the proportion of NPs of one polarity, it is possible to terminate the self-assembly process at various stages and thus control the supracrystals' sizes and solubilities. The measurements of the ζ-potential[7,8] indicate that this "termination" effect is due to the formation of protective shells of "excess" NPs around the growing aggregates; although the particles in these shells are all like-charged, the interactions between them are effectively screened and the shells are stable. The degree of the shell stability and the sizes of the crystals can be further controlled by the polydispersity of the NPs used and by the propensity of the ligands on their surfaces to form hydrogen bonds. Identification and explanation of these trends open new avenues to tailoring NP supracrystals of desired overall dimensions, stabilities, and optical characteristics.

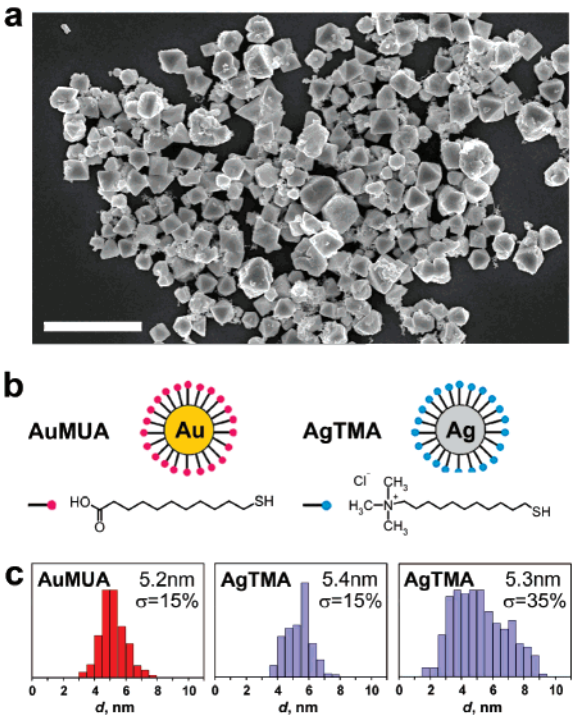

Figure 1. (a) SEM image of a typical batch of crystals prepared from oppositely charged AuMUA and AgTMA NPs (scale bar is 10 μm). (b) Scheme of AuMUA and AgTMA NPs and the structures of the coating thiols. (c) Size distributions of the metallic cores of Au (one batch) and Ag NPs (two batches) used in the experiments. Inserts give mean diameters and standard deviations (σ); statistics are based on high-resolution TEM images of at least 300 NPs from each batch.

We used gold and silver nanoparticles covered with self-assembled monolayers (SAMs[9]) of, respectively, $HS(CH_2)_{10}COOH$ [MUA] and $HS(CH_2)_{11}NMe_3^+Cl^-$ [TMA]

* Corresponding author. E-mail: grzybor@northwestern.edu. Telephone: +1-847-4913024.

10.1021/nl0701915 CCC: $37.00 © 2007 American Chemical Society
Published on Web 03/22/2007

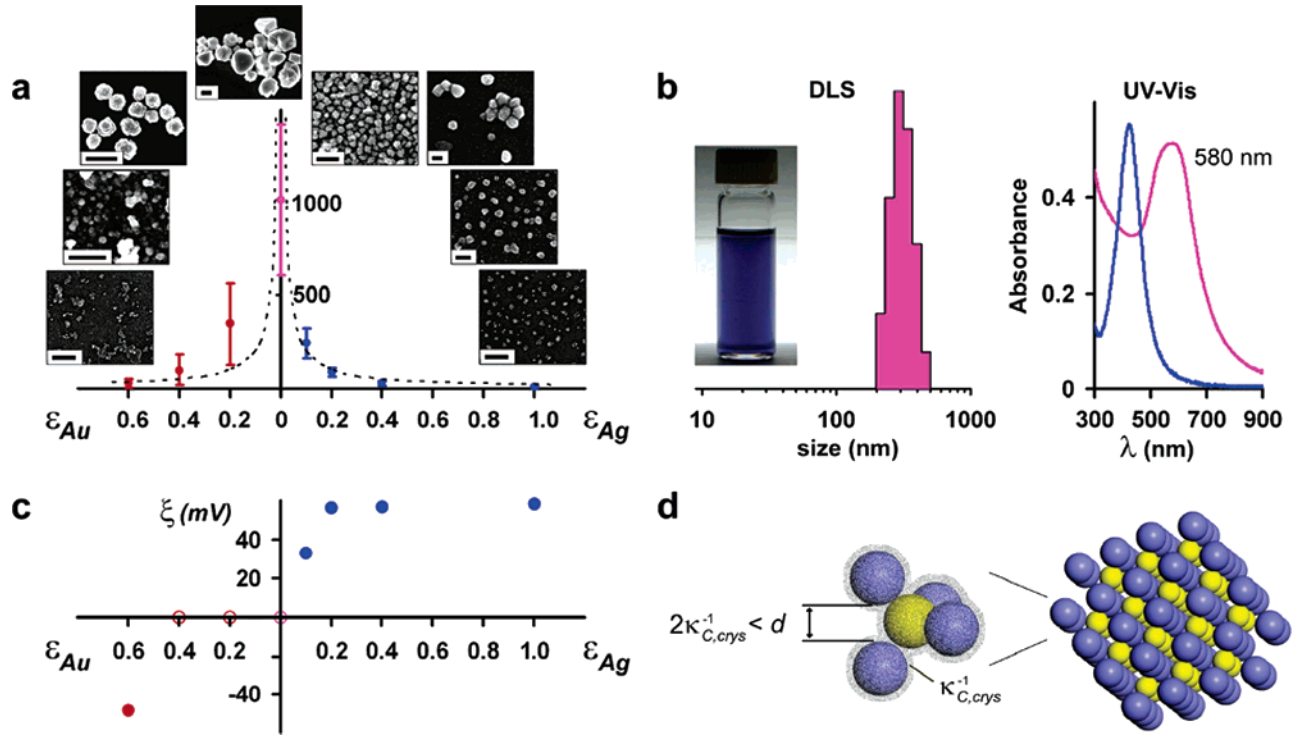

Figure 2. Crystallization of equally sized, low-dispersity (σ = 15%) 5.2 nm AuMUA and 5.4 nm AgTMA nanoparticles at pH 10. (a) Average sizes of crystals grown with different amounts of excess gold or silver NPs ($\epsilon_{Au}/\epsilon_{Ag}$, respectively). Vertical bars denote the ranges of the crystals sizes observed; insets have the SEM images of typical crystals (scale bars are 100 nm for $\epsilon_{Au} = 0.6C$ and $\epsilon_{Ag} = 0.2C$, $0.4C$, $1.0C$, and 1 μm for all other experiments). Dashed line is a theoretical fit to the expected $d \propto 1/\epsilon_{Ag}$ dependence. (b) The image on the left shows a vial containing a stable DMSO suspension of crystals grown at $\epsilon_{Ag} = 0.1C$. Middle graph has the distribution of crystal sizes determined by DLS (average size is 320 nm). The magenta line (λ_{max} = 580 nm) in the rightmost plot is the UV−vis spectrum of the crystal suspension; note the absence of the SPR band corresponding to free AgNPs (blue line, λ_{max} = 424 nm). More UV−VIS and DLS data can be found in the Supporting Information. (c) Solid markers give the values of the ζ-potential measured for soluble AuMUA/AgTMA crystals. Open markers indicate experiments in which the crystals were insolube and precipitated from solution (ζ=0). (d) Schematic representation of a AuMUA/AgTMA crystal stabilized by a shell of excess NP of either polarity. The zoom-out illustrates electrostatic screening between like charged NPs in the shell; this screening is efficient if the NP spacing is larger than ca. $2\kappa^{-1}_{C,crys}$ (for details, see refs 6 and 7).

(both thiols were obtained from ProChimia, Poland; cf. Figure 1b) and prepared as described previously.[6] The metallic cores of AuMUAs had average diameter of 5.2 nm and dispersity, σ = 15%. For AgTMAs, we used two batches with similar average core diameters (5.4 and 5.3 nm) but different dispersities (σ = 15% and σ = 35%; in the latter case, the sample contained a large proportion of smaller NPs, Figure 1c). The compositions of the NPs were estimated to be $Au_{4360}L_{400}$ and $Ag_{4880}L_{430}/Ag_{4620}L_{415}$ and corresponded to the ratio of charges on the NPs Q^+/Q^- = 1.04−1.08. We have previously shown that, with these parameters, the oppositely charged NPs assemble into diamond-like crystals several micrometers in size.[6] In the present work, we performed crystallizations according to the same procedure but varied the relative amounts of AuMUAs and AgTMAs and the values of pH (7 and 10). In a typical experiment, an electroneutral AuMUA/AgTMA solution[8] was first prepared by slowly titrating AuMUAs with AgTMAs until precipitation, washing the precipitate with water to remove salts, and then redissolving it in a 1:1 v/v DI H_2O/DMSO mixture at 60 °C to yield a 2 mM (in terms of numbers of gold and silver atoms) NP solution. A desired excess of either type of NPs was then added, and the pH of the solution was adjusted (here, to 7 or 10) by adding NMe_4OH. Crystals were grown in open plastic vials heated at 60−65 °C for 30−40 h to evaporate water and were subsequently analyzed by scanning electron microscopy (SEM) and also, if they remained in solution, by UV−vis spectroscopy, dynamic light scattering (DLS) and transmission electron microscopy (TEM).

Crystallization at High pH and at Low NP Polydispersities. When both Au and Ag NPs had comparable and relatively small dispersities (σ = 15%) (Figure 2a) and the pH = 10 was sufficiently high to deprotonate most of the COOH groups,[10] the largest crystals ($d \sim$ 1−2 micrometers in each direction) grew from electroneutral solutions, that is, from solutions of equal concentrations of NPs of the two types, $C = C_{AuMUA} = C_{AgTMA}$.

(i) Excess of AgNPs. Upon addition of an excess amount, ϵ_{Ag},[11] of AgTMAs, the average size of the crystals[12] decreased rapidly and at $\epsilon_{Ag} = C$ clusters composed of only few particles were observed. Importantly, for the assemblies with $\epsilon_{Ag} > 0$, (1) the vast majority of the excess AgTMAs were in the aggregated state as evidenced by both DLS measurements and the UV−vis spectra of the solution (no AgSPR band at $\lambda_{max} \sim$ 424 nm) (Figure 2b, see also Supporting Information), and (2) the values of the ζ (surface) potential were always positive (Figure 2c). Together, these

observations indicate that the assemblies had their outer "shells" composed mostly of the positively charged, excess AgTMAs. Despite possessing net charge, however, these shells were stable owing to the small thickness of the Debye layer[13] around the NPs ($\kappa_{C,\mathrm{crys}}^{-1} \sim 2-3$ nm) and the efficient screening of energetically unfavorable repulsions between NPs spaced by $d > 2\kappa_{C,\mathrm{crys}}^{-1}$ (Figure 2d). In the context of self-assembly, the shells not only stabilized[7] the isolated clusters/aggregates (through mutual electrostatic repulsions) but also controlled their ultimate sizes (through the amount of available excess NPs, ϵ_{Ag}). Indeed, because the number of NPs in a crystal of characteristic dimension d scales as d^3, while the number of NPs necessary to build a protective shell around it scales with d^2, the sizes of crystals should scale (assuming all AgTMAs are used; cf. point 1 above) inversely with ϵ_{Ag} (i.e., $d \sim 1/\epsilon_{\mathrm{Ag}}$). As shown in Figure 2a, this prediction is in qualitative agreement with our experimental results.

Because the charged shells stabilized the solution phase, they rendered crystals smaller than ~300−400 nm ($\epsilon_{\mathrm{Ag}} \geq 0.1C$) soluble. This threshold size agrees with the predictions based on the DLVO (Deryaguin−Landau−Verwey−Overbeek) theory according to which colloidal stability is governed by an interparticle potential $V_{\mathrm{tot}}(r)$ composed of Coulombic, $V_{\mathrm{el}}(r)$, and van der Waals, $V_{\mathrm{vdW}}(r)$, contributions.[14] For a relatively thin Debye screening layer (like the one in our system) and for low surface potential ψ_0, the energy of electrostatic repulsion between like-charged particles (here, crystals)[15] of size a and separated by distance r can be approximated as $V_{\mathrm{el}}(r) = 2\pi\epsilon\epsilon_0 a\psi_0^2 \ln(1 + \exp(-\kappa_{C,\mathrm{sol}}r))$, where ϵ is the dielectric constant of the solvent, ϵ_0 stands for the dielectric permittivity of vacuum, and $\kappa_{C,\mathrm{sol}}^{-1}$ denotes the Debye length.[16,17] On the other hand, the attractive vdW potential can be written as $V_{\mathrm{vdW}}(r) = -A/6[2a^2/r(4a + r) + 2a^2/(2a + r)^2 + \ln(r(4a + r)/(2a + r)^2)]$, where A is a Hamaker constant. Importantly, the sum of these two potentials has a local maximum ("barrier") that the crystals need to overcome in order to aggregate. For the values of parameters corresponding to those used in experiment, $\kappa_{C,\mathrm{sol}}^{-1} = 19$ nm (in 2×10^{-4} M solution of NMe_4OH, pH 10), measured potential $\psi_0 \sim 32$ mV, $A \approx 4.25 \times 10^{-19}$ J for gold and silver surfaces taken as the average of the Au−Au and Ag−Ag Hamaker constants,[18] and $\epsilon_{\mathrm{DMSO}} = 48$; this maximum is located at $r(V_{\mathrm{tot}}^{\mathrm{max}}) \approx 30$ nm and can be overcome by the thermal energy of the crystals, $3/2kT$, provided that they are larger than $a_{\mathrm{crit}} \sim 380$ nm. In other words, for crystals larger than a_{crit}, $V_{\mathrm{tot}}^{\mathrm{max}} < 3/2\ kT$ and the crystals aggregate/precipitate; for crystals smaller than a_{crit}, $V_{\mathrm{tot}}^{\mathrm{max}} > 3/2\ kT$ and the crystals are stable in solution, in agreement with experimental observations.[19]

(ii) Excess of AuNPs. With the addition of excess AuMUAs, ϵ_{Au}, the overall trends were qualitatively similar, but the crystalline aggregates were not as well defined as with excess silver. The ordered domains were often connected to one another within larger structures, and for $\epsilon_{\mathrm{Au}} \geq 0.4C$, the clusters formed a continuous (amorphous) phase. This behavior is likely due to residual hydrogen bonding between the AuMUA shells (because, at pH = 10, ~1% of the carboxylic groups are still protonated[10]), which competes with electrostatic forces and promotes NP flocculation rather than crystallization.[6]

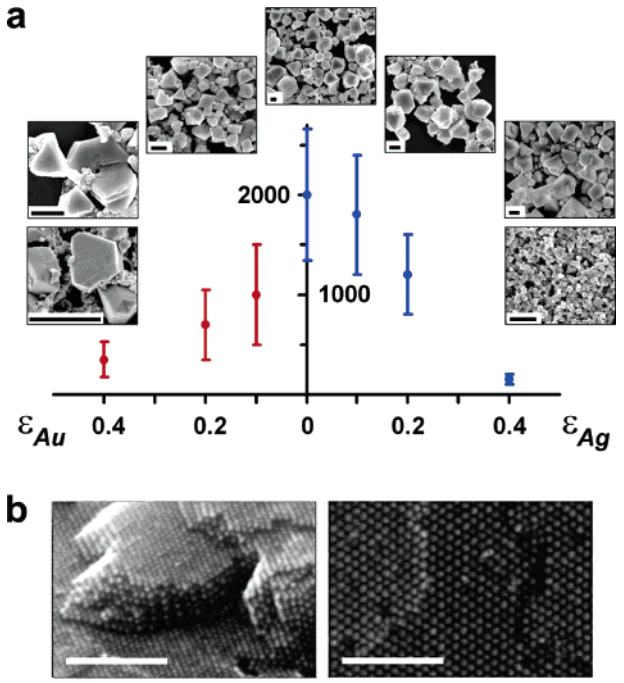

Figure 3. Supracrystals grown at pH = 10 from mixtures of low dispersity AuMUAs (5.2 nm, σ = 15%) and high dispersity AgTMAs (5.3 nm, σ = 35%). (a) Average sizes of crystals obtained with various amounts of excess Au or Ag NPs. Vertical bars denote the range of the crystals' sizes; inserts give SEM images of typical crystals; scale bars are all 1 μm. (b) SEM images of typical crystal faces illustrate that although the crystallizing solutions contain large proportion of small AgNPs, the resulting crystals incorporate only particles from a narrow size distribution (5.3 ± 0.5 nm). Scale bars in both pictures are 100 nm.

Effects of NP Polydispersity. At pH = 10 but with the dispersity of the AgTMA NPs increased to σ = 35%, large ($d \sim 2-3$ μm), good quality crystals were obtained within a wider range of relative NP concentrations, from $\epsilon_{\mathrm{Ag}} \sim 0.2C$ to $\epsilon_{\mathrm{Au}} \sim 0.2C$ (Figure 3a). To explain this effect, we first note that despite the presence of a large fraction of small AgNPs (cf. Figure 1c), the particles forming the crystals were all of very similar sizes close to the average (5.3 ± 0.5 nm by SEM; Figure 3b). At the same time, TEM images of the solution phase (drop cast onto a copper grid) showed a large proportion (>70%) of the smaller, 2−4 nm, free AgNPs. As we have suggested previously,[6] the possible role of these small particles was to screen the electrostatic interactions between large (crystallizing) NPs, thus lowering the chemical potential of the dispersed phase, preventing flocculation, and promoting crystallization. Of course, when the excess of the NPs of either polarity was large (ϵ_{Au}, $\epsilon_{\mathrm{Ag}} \geq 0.2C$), it offset these stabilizing effects, and the crystals' dimensions and quality (i.e., smoothness of faces, regularity of shapes) decrease rapidly.

Effects of pH. Finally, we discuss briefly the most complex situation in which polydispersity of the sample, the electrostatic forces, and hydrogen bonding between MUA SAMs (pH = 7 slightly below the pK_a of the MUA SAM)

were all operative. Under these conditions, the crystals were of poor quality and had multiple defects and twinnings. Furthermore, addition of excess NPs not only decreased average crystal size but also led to the formation of interconnected polycrystalline aggregates (especially when AuMUAs were in excess). These effects can be attributed to the competition between electrostatic forces that drive crystallization and NP−NP hydrogen bonding, which weakens electrostatic MUA−MUA repulsions and drives aggregation. In addition, for $\epsilon_{Au} > 0$, protonation of MUA carboxylic groups lowers the effective charge of the shells that are supposed to "passivate" the growing crystals; this, in turn, increases the chemical potential[6] of the isolated aggregates in solution and causes their flocculation into interconnected crystallites.

In summary, this work demonstrates that (i) largest and highest quality "ionic" supracrystals grow from fully ionized NPs in the absence of other types of "competing" interactions (e.g., H-bonding), and (ii) the sizes of the crystals can be controlled in a straightforward fashion by adding excess NPs of either polarity. In the future, it would be interesting to generalize and quantify these observations for supracrystals made of nanoobjects of different sizes and material properties. In particular, charge-stabilized, soluble supracrystals made of different combinations of fluorescent/luminescent NPs might provide a new route to "composite" nano/microparticles of tunable optical properties.

Acknowledgment. This work was supported by the ACS PRF grant (no. 0965-350-a240). B.A.G. gratefully acknowledges financial support from 3M, the Alfred P. Sloan Fellowship, and the Pew Scholars Program.

Supporting Information Available: Experimental details of nanoparticle synthesis, UV−vis, DLS, ζ-potential measurements, and high-resolution SEM images. This material is available free of charge via the Internet at http://pubs.acs.org.

References

(1) Stellacci, F. *Nat. Mater.* **2005**, *4*, 113.
(2) Maier, S. A.; Kik, P. G.; Atwater, H. A.; Meltzer, S.; Harel, E.; Koel, B. E.; Requicha, A. A. G. *Nat. Mater.* **2003**, *2*, 229.
(3) Hoinville, J.; Bewick, A.; Gleeson, D.; Jones, R.; Kasyutich, O.; Mayes, E.; Nartowski, A.; Warne, B.; Wiggins, J.; Wong, K. *J. Appl. Phys* **2003**, *93*, 7187.
(4) Grunes, J.; Zhu, J.; Anderson, E. A.; Somorjai, G. A. *J. Phys. Chem. B* **2002**, *106*, 11463.
(5) Zayats, M.; Kharitonov, A. B.; Pogorelova, S. P.; Lioubashevski, O.; Katz, E.; Willner, I. *J. Am. Chem. Soc.* **2003**, *125*, 16006.
(6) Kalsin, A. M.; Fialkowski, M.; Paszewski, M.; Smoukov, S. K.; Bishop, K. J. M.; Grzybowski, B. A. *Science* **2006**, *312*, 420.
(7) Kalsin, A. M.; Pinchuk, A. O.; Smoukov, S. K.; Paszewski, M.; Schatz, G. C.; Grzybowski, B. A. *Nano Lett.* **2006**, *6*, 1896.
(8) Kalsin, A. M.; Kowalczyk, B.; Smoukov, S. K.; Klajn, R.; Grzybowski, B. A. *J. Am. Chem. Soc.* **2006**, *128*, 15046.
(9) Witt, D.; Klajn, R.; Barski, P.; Grzybowski, B. A. *Curr. Org. Chem.* **2004**, *8*, 1763.
(10) The pK_a of a MUA SAM on curved/corrugated surfaces have been estimated to be about 8; cf. Leopold, M. C.; Black J. A.; Bowden, E. F. *Langmuir* **2002**, *18*, 978; Smalley, J. F. *Langmuir* **2003**, *19*, 9284. Therefore, at pH = 10, approximately 1% of the carboxylic groups on the surface of MUA NPs are protonated.
(11) The value of ϵ for the NPs present in excess is defined as abs($c_{Au} - c_{Ag}$)/min(c_{Au},c_{Ag}), where c denotes NP concentrations. For example, if the solution is 3 mM in AgTMA and 2 mM in AuMUA, ϵ_{Ag} = abs(2−3)/min(2,3) = 0.5.
(12) The powder XRD spectra of the large, micron-sized crystals obtained at low values of $\epsilon \sim 0-0.05$ gave peaks at locations 0.801°, 1.308°, and 1.539°. These peaks corresponded to {111}, {220}, and {311} Bragg reflections of the diamond-like (sphalerite) lattice. For crystals smaller than few hundreds of nm, XRD method did not yield resolvable spectrum, as these crystals had more deformations and defects (for representative examples of HRSEM images, please see Supporting Information, Figure S3).
(13) The calculation of the thickness of the Debye layer around the NPs *in* the crystals is based on the previously published (cf. ref 6) EDS measurements of the counterions' concentration. Importantly, this concentration is higher in the crystal than in the surrounding solution by ca. 100 times, hence $\kappa_{C,crys}^{-1} = 2-3$ nm $< \kappa_{C,sol}^{-1} \approx 19$ nm.
(14) Israelachvili, J. N. *Intermolecular and Surface Forces*, 2nd ed.; Academic Press: San Diego, 1992.
(15) In these calculations, we approximate supracrystals as roughly spherical.
(16) Hunter, R. J. *Foundations of Colloid Science*; Clarendon Press: Oxford, 1995.
(17) Overbeek, J. T. G. *J. Colloid Interface Sci.* **1977**, *58*, 408.
(18) Visser, J. *Adv. Colloid Interface Sci.* **1972**, *3*, 331.
(19) Crystals near the threshold size (300−400 nm; $\epsilon_{Ag} \sim 0.1C$) precipitate within one to two days. Smaller crystals/clusters ($\epsilon_{Ag} \sim 0.2-1.0C$) are stable in solution for weeks.

NL0701915